

Structural and thermoelectric properties of $\text{Bi}_2\text{Sr}_2\text{Co}_2\text{O}_y$ thin films on LaAlO_3 (100) and fused silica substrates

Shufang Wang, A. Venimadhav, Shengming Guo, Ke Chen, Qi Li, A. Soukiassian, Darrell G. Schlom, Michael B. Katz, X. Q. Pan, Winnie Wong-Ng, Mark D. Vaudin, and X. X. Xi

Citation: *Applied Physics Letters* **94**, 022110 (2009); doi: 10.1063/1.3072803

View online: <http://dx.doi.org/10.1063/1.3072803>

View Table of Contents: <http://scitation.aip.org/content/aip/journal/apl/94/2?ver=pdfcov>

Published by the *AIP Publishing*

Articles you may be interested in

Enhanced high temperature thermoelectric properties of Bi-doped c-axis oriented $\text{Ca}_3\text{Co}_4\text{O}_9$ thin films by pulsed laser deposition

J. Appl. Phys. **108**, 083709 (2010); 10.1063/1.3499324

Effect of Li doping in NiO thin films on its transparent and conducting properties and its application in heteroepitaxial p-n junctions

J. Appl. Phys. **108**, 083715 (2010); 10.1063/1.3499276

Epitaxial growth and transport properties of $\text{Bi}_2\text{Sr}_2\text{Co}_2\text{O}_y$ thin films by metal organic deposition

Appl. Phys. Lett. **94**, 162108 (2009); 10.1063/1.3122930

Thermoelectric properties and microstructure of c-axis-oriented $\text{Ca}_3\text{Co}_4\text{O}_9$ thin films on glass substrates

Appl. Phys. Lett. **87**, 171912 (2005); 10.1063/1.2117615

Influence of pulsed laser deposition growth conditions on the thermoelectric properties of $\text{Ca}_3\text{Co}_4\text{O}_9$ thin films

J. Appl. Phys. **97**, 013706 (2005); 10.1063/1.1823582



You don't still use this cell phone

or this computer

Why are you still using an AFM designed in the 80's?

It is time to upgrade your AFM

Minimum \$20,000 trade-in discount for purchases before August 31st

Asylum Research is today's technology leader in AFM

dropmyoldAFM@oxinst.com

OXFORD
INSTRUMENTS
The Business of Science®

Structural and thermoelectric properties of $\text{Bi}_2\text{Sr}_2\text{Co}_2\text{O}_y$ thin films on LaAlO_3 (100) and fused silica substrates

Shufang Wang,^{1,2,a)} A. Venimadhav,^{1,3} Shengming Guo,^{1,4} Ke Chen,¹ Qi Li,¹ A. Soukiasian,² Darrell G. Schlom,² Michael B. Katz,⁵ X. Q. Pan,⁵ Winnie Wong-Ng,⁶ Mark D. Vaudin,⁶ and X. X. Xi^{1,2}

¹Department of Physics, The Pennsylvania State University, University Park, Pennsylvania 16802, USA

²Department of Materials Science and Engineering, The Pennsylvania State University, University Park, Pennsylvania 16802, USA

³Cryogenic Engineering Centre, IIT Kharagpur, Kharagpur-721302, India

⁴Department of Physics, Tsinghua University, Beijing 100084, People's Republic of China

⁵Department of Materials Science and Engineering, University of Michigan, Ann Arbor, Michigan 48109, USA

⁶Ceramic Division, National Institute of Standards and Technology, Gaithersburg, Maryland 20899, USA

(Received 8 October 2008; accepted 29 December 2008; published online 15 January 2009)

We have grown $\text{Bi}_2\text{Sr}_2\text{Co}_2\text{O}_y$ thin films on LaAlO_3 (100) and fused silica substrates by pulsed laser deposition. The films on LaAlO_3 are *c*-axis oriented and partially in-plane aligned with multiple domains, while the films on fused silica are preferred *c*-axis oriented without in-plane alignment. The Seebeck coefficient and resistivity of films on both substrates are comparable to those of single crystals. An oxide *p*-*n* heterojunction was formed by depositing $\text{Bi}_2\text{Sr}_2\text{Co}_2\text{O}_y$ film on Nb-doped SrTiO_3 single crystal, which showed a rectifying behavior. These thin films and heterostructures may be used for future thermoelectric applications. © 2009 American Institute of Physics.

[DOI: 10.1063/1.3072803]

Layered cobalt oxides have attracted great attention as a promising candidate for thermoelectric applications since the discovery of large Seebeck coefficient and relatively low resistivity in Na_xCoO_2 .^{1,2} Among various layered cobalt oxides,^{3–11} $\text{Bi}_2\text{Sr}_2\text{Co}_2\text{O}_y$ shows a high thermoelectric figure of merit $ZT=S^2T/(\rho\kappa)$ of ~ 1.1 at over 700 °C,¹² where *S* is the Seebeck coefficient, *T* is the temperature, ρ is the electric resistivity, and κ is the thermal conductivity. Similar to Na_xCoO_2 , $\text{Bi}_2\text{Sr}_2\text{Co}_2\text{O}_y$ has a layered structure consisting of misfit layers of triangular Co–O planes and square lattice planes of the other metal oxide. The CdI₂-type CoO_2 subcell, in which electrons are strongly correlated, serves as electronic transport layers to achieve the large Seebeck coefficient and low electric resistivity, while the distorted rocksalt-type $\text{Bi}_2\text{Sr}_2\text{O}_4$ subcell enhances phonon scattering to achieve the low thermal conductivity.³ $\text{Bi}_2\text{Sr}_2\text{Co}_2\text{O}_y$ single crystal and polycrystalline bulk samples have been studied, and $S_{ab} \sim 130$ V/K and $\rho_{ab} \sim 6$ mΩ cm were reported for single crystals at room temperature.³ Many thermoelectric applications such as thermochemistry-on-a-chip, DNA microarrays, fiber-optic switches, and microelectrothermal systems have been cited for thermoelectric thin films.¹³ So far, no $\text{Bi}_2\text{Sr}_2\text{Co}_2\text{O}_y$ thin films have been reported. In this paper we report structural and thermoelectric properties of $\text{Bi}_2\text{Sr}_2\text{Co}_2\text{O}_y$ thin films grown by pulsed laser deposition (PLD). The excellent properties in these films open up tremendous opportunities for future thermoelectric applications.

$\text{Bi}_2\text{Sr}_2\text{Co}_2\text{O}_y$ thin films were grown by PLD from a ceramic $\text{Bi}_2\text{Sr}_2\text{Co}_2\text{O}_y$ target on (100) oriented single crystal LaAlO_3 and amorphous fused silica substrates. The fused silica substrate has low thermal conductivity, an additional advantage for thermoelectric applications. An excimer laser

with 248 nm radiation was used for PLD with a laser energy density of 1.5 J/cm² and a repetition rate of 3 Hz. An oxygen pressure of 40 Pa (300 mTorr) was maintained during the film growth at substrate temperatures of 690–730 °C. The deposition rate was ~ 0.18 nm/pulse. After the deposition, the films were cooled to room temperature within 5 min in 8×10^4 Pa (600 Torr) oxygen. Energy dispersive x-ray spectroscopy analysis of different spots on the surface of a film showed a Bi:Sr:Co ratio of 1.00:1.08:0.95 with an error of about 10%.

Figure 1(a) shows a typical x-ray diffraction (XRD) θ -2 θ scan of $\text{Bi}_2\text{Sr}_2\text{Co}_2\text{O}_y$ thin films on (1 0 0) LaAlO_3 taken on a Philips X'Pert Pro MRD four-circle diffractometer with Cu *K*α radiation. Only peaks from diffractions of (00*l*) $\text{Bi}_2\text{Sr}_2\text{Co}_2\text{O}_y$ planes were observed besides the substrate peaks, indicating that the film is *c*-axis oriented. The ω -scan of the $\text{Bi}_2\text{Sr}_2\text{Co}_2\text{O}_y$ (0 0 16) peak showed a full width at half maximum of 0.4°, further confirming the excellent *c*-axis orientation of the film. The θ -2 θ scan for the $\text{Bi}_2\text{Sr}_2\text{Co}_2\text{O}_y$ film on amorphous fused silica is shown in Fig. 1(b). In addition to strong $\text{Bi}_2\text{Sr}_2\text{Co}_2\text{O}_y$ (00*l*) reflections, there are several weak peaks representative of other orientations. We calculated the degree of *c*-axis orientation *A* by using the equation $A=(P-P_0)/(1-P_0)$, where $P=\sum I_{(00l)}/\sum I_{(hkl)}$ is for films and P_0 for the random oriented powders (*I* is the peak intensity of a Bragg reflection) and an *A* value of 1 corresponds to a perfect *c*-axis orientation.¹⁴ We find that *A* for the film on fused silica is about 0.75.

The *ab*-plane texture information was investigated by XRD pole figures using a Bruker D8 diffractometer with the general area detector diffraction system (GADDS) system. Figure 2(a) shows the result for a $\text{Bi}_2\text{Sr}_2\text{Co}_2\text{O}_y$ thin film on LaAlO_3 (001) substrate. For the 2 0 8, 1 1 12, and 0 2 10 reflections, 12 spots overlap with the continuous Debye rings, indicating the existence of three different in-plane ori-

^{a)}Electronic mail: suw16@psu.edu.

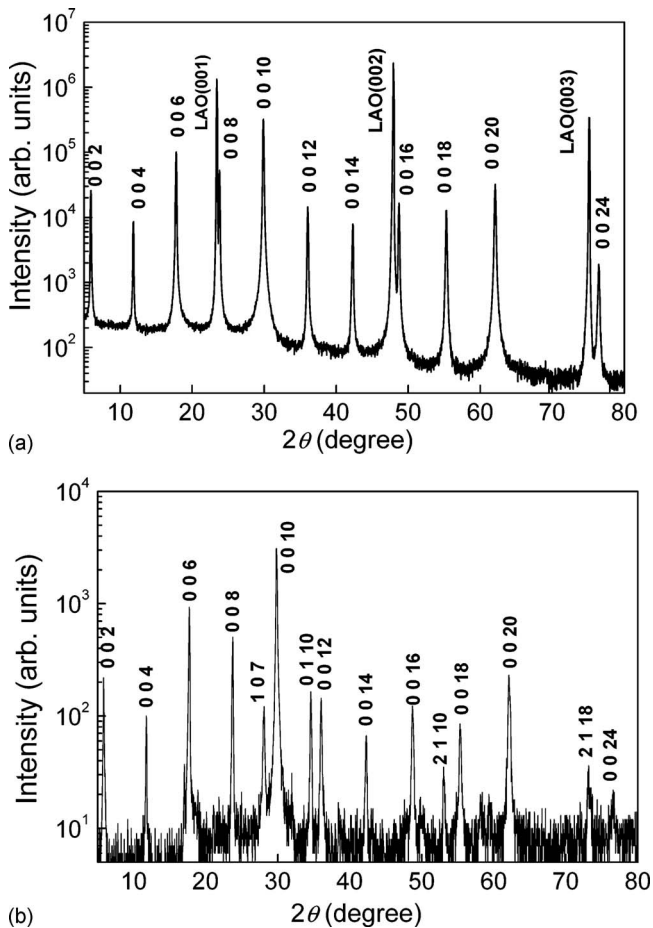


FIG. 1. XRD θ - 2θ scans of the $\text{Bi}_2\text{Sr}_2\text{Co}_2\text{O}_y$ thin films on (a) LaAlO_3 (001) and (b) fused silica substrates.

ented domains aligned 30° apart from each other in addition to randomly oriented regions. The small splitting of these spots was due to the small differences in the a (0.4911 nm) and b (0.5111 nm) lattice parameters. The Debye rings for a $\text{Bi}_2\text{Sr}_2\text{Co}_2\text{O}_y$ thin film on fused silica substrate are continuous and smooth, indicating that the film is polycrystalline, fine grained, and has no in-plane texture. Figure 2(b) is a cross-sectional high-resolution transmission electron microscopy (HRTEM) image of a $\text{Bi}_2\text{Sr}_2\text{Co}_2\text{O}_y$ film on LaAlO_3 (001) substrate performed on a JEOL 3011 HRTEM system. Different layers within the film, as well as superlattice structures within the layers, are clearly visible in the image. The light band in the image shows the existence of regions of

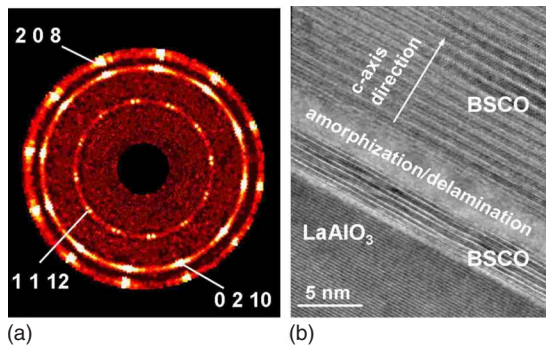


FIG. 2. (Color online) (a) Pole figure of the $\text{Bi}_2\text{Sr}_2\text{Co}_2\text{O}_y$ thin film on LaAlO_3 (001) substrate and (b) HRTEM image of the $\text{Bi}_2\text{Sr}_2\text{Co}_2\text{O}_y/\text{LaAlO}_3$ interface.

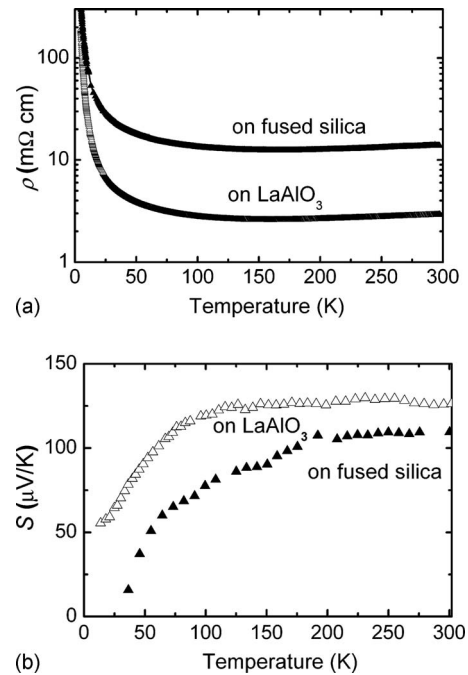


FIG. 3. The temperature dependence of (a) resistivity and (b) Seebeck coefficient for the $\text{Bi}_2\text{Sr}_2\text{Co}_2\text{O}_y$ thin films on LaAlO_3 (001) and fused silica substrates.

amorphization or delamination in the film. These structural defects provide additional scattering to electron and phonon transport, which will influence the thermoelectric properties of the film.

The resistivity versus temperature curves for two 300 nm thick $\text{Bi}_2\text{Sr}_2\text{Co}_2\text{O}_y$ thin films on LaAlO_3 (001) and fused silica substrates ($5 \times 5 \text{ mm}^2$ in size) are shown in Fig. 3(a), measured using a van der Pauw geometry on a dip probe inside a liquid helium tank. A metal-insulator transition is observed at about 140 K, which has been attributed to the decrease in the effective carrier number due to a pseudogap formation.¹⁵ The room temperature resistivity for film on LaAlO_3 is about 3 m Ω cm, similar to the ab -plane resistivity of $\text{Bi}_2\text{Sr}_2\text{Co}_2\text{O}_y$ single crystal and much smaller than that of the polycrystalline bulk.^{3,16} The room temperature resistivity for the film on fused silica is larger possibly due to the much larger c -axis resistivity than the ab -plane resistivity¹⁷ and the polycrystalline nature of the films. The Seebeck coefficient was measured using a Quantum Design physical properties measurement system (PPMS) system with a thermal transport option. The measurement was carried out in vacuum (10^{-5} Pa) with a four-probe steady-state mode. The sample was 3 mm wide and 10 mm long. A resistive heater was connected to one end of the film, while the other end was mounted on a cold sink. The temperature gradient was measured by two thin film Cernox chip thermometers, and it was maintained at typically 0.5 K for the measurement. Figure 3(b) shows the temperature dependence of Seebeck coefficient for two 300 nm thick $\text{Bi}_2\text{Sr}_2\text{Co}_2\text{O}_y$ thin films on LaAlO_3 and fused silica substrates. The temperature dependence is similar to those of other layered cobalt oxides such as Na_xCoO_2 and $\text{Ca}_3\text{Co}_4\text{O}_9$,^{1,8,9} and the positive S values indicate a hole transport. The room temperature S of the film is about 125 $\mu\text{V}/\text{K}$ on LaAlO_3 and 110 $\mu\text{V}/\text{K}$ on fused silica. They are close to the single crystal value of

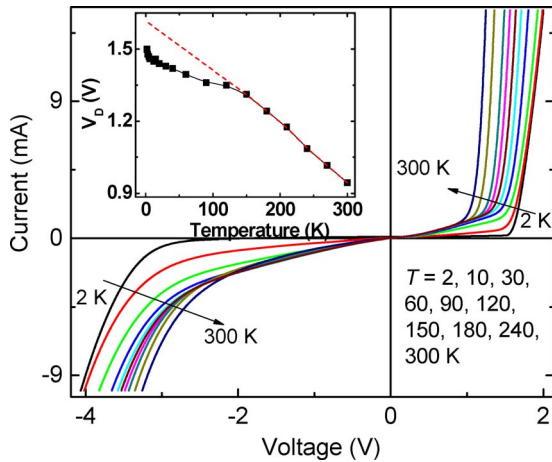


FIG. 4. (Color online) Current-voltage characteristics of $\text{Bi}_2\text{Sr}_2\text{Co}_2\text{O}_y/\text{Nb-doped SrTiO}_3$ heterojunction measured from 2 to 300 K. The inset shows the temperature-dependent diffusion voltage of the $\text{Bi}_2\text{Sr}_2\text{Co}_2\text{O}_y/\text{Nb-doped SrTiO}_3$ heterojunction.

130 $\mu\text{V}/\text{K}$ and much higher than 60 $\mu\text{V}/\text{K}$ in bulk polycrystalline samples.^{3,16}

While the resistivity and Seebeck coefficient presented here are the in-plane properties of the films, the *ab*-plane thermal conductivity k_{ab} is difficult to measure for a thin film sample. The through thickness thermal conductivity k_c of a film on a LaAlO_3 substrate was measured by the time-domain thermoreflectance technique.¹⁸ A value of 0.45 $\text{W}/\text{m K}$ was obtained at room temperature, which is close to the single crystal value of ~ 0.4 $\text{W}/\text{m K}$.¹⁹ If we used the single crystal k_{ab} value of 2 $\text{W}/\text{m K}$,³ the *ZT* for the *c*-axis oriented film on LaAlO_3 substrate is about 0.08 at room temperature, which is higher than $ZT \sim 0.05$ in single crystals due to slightly lower resistivity.¹² We were not able to measure the thermoelectric properties of the films at high temperatures, but since the *ZT* value of $\text{Bi}_2\text{Sr}_2\text{Co}_2\text{O}_y$ single crystal increases from ~ 0.05 at room temperature to ~ 1.1 at 700 $^\circ\text{C}$,¹² we can expect high *ZT* values in the $\text{Bi}_2\text{Sr}_2\text{Co}_2\text{O}_y$ films at high temperatures.

A 140 nm thick $\text{Bi}_2\text{Sr}_2\text{Co}_2\text{O}_y$ layer was deposited on Nb-doped (0.7 wt %) SrTiO_3 single crystal, which is a *n*-type thermoelectric material.²⁰ XRD pattern of the layer showed single phase and *c*-axis oriented growth. Since the charge carrier in $\text{Bi}_2\text{Sr}_2\text{Co}_2\text{O}_y$ is *p* type, the $\text{Bi}_2\text{Sr}_2\text{Co}_2\text{O}_y/\text{Nb-doped SrTiO}_3$ structure forms a *p-n* heterojunction. Figure 4 presents the *I-V* curves of the heterojunction from 2 to 300 K, in which a strong asymmetry indicates a rectifying property. The temperature dependence of the diffusion voltage V_D , defined by the forward voltage corresponding to the rapid current increase in the *I-V* curves, is shown in the inset of Fig. 4. At high temperatures V_D increases linearly with decreasing temperature and then deviates from this behavior below the metal-insulator transition

temperature of the $\text{Bi}_2\text{Sr}_2\text{Co}_2\text{O}_y$ layer. The deviation may be explained by the formation of the pseudogap in $\text{Bi}_2\text{Sr}_2\text{Co}_2\text{O}_y$ below the metal-insulator transition.²¹

In conclusion, *c*-axis oriented $\text{Bi}_2\text{Sr}_2\text{Co}_2\text{O}_y$ thin films with multidomain in-plane texturing have been grown on single crystal LaAlO_3 (001) substrate by PLD, while the films on fused silica substrates are preferred *c*-axis oriented without in-plane texture. The Seebeck coefficient and resistivity of the films on both substrates are very similar to those in single crystal samples. The *p-n* heterojunction using the $\text{Bi}_2\text{Sr}_2\text{Co}_2\text{O}_y/\text{Nb-doped SrTiO}_3$ structure shows a rectifying property. The availability of these thin films and heterostructures opens up opportunities for various thermoelectric applications.

We thank Professor Terasaki for stimulating discussions that initiated this work. The thermal conductivity of a film was measured in Professor Cahill's laboratory at the U. Illinois, for which we acknowledge gratefully. This work was partially supported by DOE under Grant No. DE-FG02-01ER45907 (X.X.X.) and NSF under Grant Nos. DMR-0405502 (Q.L.), DMR-0507146 (D.G.S. and X.X.X.), and DMR-0315633 (X.Q.P.).

- ¹I. Terasaki, Y. Sasago, and K. Uchinokura, *Phys. Rev. B* **56**, R12685 (1997).
- ²R. E. Schaak, T. Klimczuk, M. L. Foo, and R. J. Cava, *Nature (London)* **424**, 527 (2003).
- ³K. Koumoto, I. Terasaki, and R. Funahashi, *MRS Bull.* **31**, 206 (2006).
- ⁴R. Funahashi and M. Shikano, *Appl. Phys. Lett.* **79**, 362 (2001).
- ⁵W. Kobayashi and I. Terasaki, *Appl. Phys. Lett.* **89**, 072109 (2006).
- ⁶D. Pelloquin, S. Hebert, A. Maignan, and B. Raveau, *J. Solid State Chem.* **178**, 769 (2005).
- ⁷S. Hebert, S. Lambert, D. Pelloquin, and A. Maignan, *Phys. Rev. B* **64**, 172101 (2001).
- ⁸M. Shikano and R. Funahashi, *Appl. Phys. Lett.* **82**, 1851 (2003).
- ⁹A. C. Masset, C. Michel, A. Maignan, M. Hervieu, O. Toulemonde, F. Studer, B. Raveau, and J. Hejtmanek, *Phys. Rev. B* **62**, 166 (2000).
- ¹⁰A. Sakai, T. Kanno, S. Yotsuhashi, S. Okada, and H. Adachi, *J. Appl. Phys.* **99**, 093704 (2006).
- ¹¹H. H. Yamauchi, K. Sakai, T. Nagai, Y. Matsui, and M. Karppinen, *Chem. Mater.* **18**, 155 (2006).
- ¹²I. Terasaki, The European Multifunctional Materials Workshop, Haaholmen, Norway, 17–21 June 2007 (unpublished).
- ¹³R. Venkatasubramanian, E. Siivola, T. Colpitts, and B. O'Quinn, *Nature (London)* **413**, 597 (2001).
- ¹⁴F. K. Lotgering, *J. Inorg. Nucl. Chem.* **9**, 113 (1959).
- ¹⁵T. Itoh and I. Terasaki, *Jpn. J. Appl. Phys., Part 1* **39**, 6658 (2000).
- ¹⁶R. Funahashi, I. Matsubara, and S. Sodeoka, *Appl. Phys. Lett.* **76**, 2385 (2000).
- ¹⁷T. Yamamoto, K. Uchinokura, and I. Tsukada, *Phys. Rev. B* **65**, 184434 (2002).
- ¹⁸D. G. Cahill, *Rev. Sci. Instrum.* **75**, 5119 (2004).
- ¹⁹I. Terasaki, H. Tanaka, A. Satake, S. Okada, and T. Fujii, *Phys. Rev. B* **70**, 214106 (2004).
- ²⁰S. Ohta, T. Nomura, H. Ohta, and K. Koumoto, *J. Appl. Phys.* **97**, 034106 (2005).
- ²¹I. Terasaki, *Mater. Trans., JIM* **42**, 951 (2001).